X-645-72-201

DOUBLE FLOATING PROBE MEASUREMENTS ON S^3A

NELSON C. MAYNARD
DAVID P. CAUFFMAN

JUNE 1972

GSFC — GODDARD SPACE FLIGHT CENTER —
GREENBELT, MARYLAND

DOUBLE FLOATING PROBE MEASUREMENTS ON S-3A

Nelson C. Maynard
and
David P. Cauffman*

Goddard Space Flight Center
Greenbelt, Maryland 20771

*NAS-NRC Research Associate; Present Address:
Plasma Research Lab., Aerospace Corp.,
El Segundo, California 90245

(To be submitted to J.G.R.)

DOUBLE FLOATING PROBE MEASUREMENTS ON S^3-A

S^3-A (Explorer 45) was launched into an eccentric equatorial orbit with a 5.2 R_e apogee and 3^o inclination on November 11, 1971 (see Longanecker and Hoffman, 1972, for a description of the spacecraft and its experiment complement). The spacecraft carried a pair of symmetrical floating probes designed to measure D.C. electric fields in regions well inside the plasmapause. The sensors are 5.5" diameter spheres on fiberglass fold-out booms separated by a distance of 5.08 meters. The plasma sheath surrounding the spacecraft is asymmetrical since only one side of the satellite is photoemitting and the sunlit surface is non-conducting. At high altitudes the sheath engulfs the spheres preventing measurements of D.C. electric fields. Responding to sheath potentials in these regions, the probes become sensitive to ambient temperature and density changes which control the sheath parameters. The experiment can therefore serve as a crude plasmapause detector. The purpose of this letter is to introduce results from model calculations made to explain the observed probe potential behavior, to use these and comparisons with VLF data to establish that certain effects seen are interpretable as the plasmapause, and to present the behavior of the plasmapause during and around the December 17, 1971 magnetic storm using the double-probe data.

In Figure 1 raw data, sampled spin synchronously and shown expanded in the inserts, is displayed for part of an outbound pass from R_e = 1.5 to 4.1. The data may be divided into three regions. The first region, represented by the left insert, has a decreasing amplitude,

sinusoidal waveform resulting from measurement of $\vec{V} \times \vec{B}$ and any ambient electric fields in the spin plane. At the far right (~14:42 U.T.) of Figure 1 the experiment output saturates at the point we are identifying as the plasmapause. After about 13:40 U.T. the experiment is being affected by sheath potentials. As seen from the center and right inserts these potentials often distort the waveform and may result in the occurrence of the waveform maximum either simultaneous with the roll start (arrows in figure) or one half roll later. The orientation of the antennas is toward or away from the sun, the sunward probe being more negative in the case shown in the right insert and more positive in the case of the center insert. Typically, with increasing altitude, the sheath potentials begin to affect the probes first in the 'negative mode' (sunward sphere more negative), then may switch modes (sometimes several times) and finally end up in the 'negative mode' just prior to and during saturation.

In order to explain the above observations a model has been created in which the system is divided into four floating Langmuir probes. The interaction between the probes is computed considering space charge effects and exchange currents and iteratively solving the four resultant non-linear, infinite-degree equations specified by current balance requirements. Figure 2 shows schematically the coupled system with probes 1 and 2 being the spheres and probes 3 and 4 being the sunlit and dark hemispheres respectively of the spacecraft, (approximated by a spherical shape). A comprehensive paper on the model is now in preparation. The solution has been attempted only for the antenna

axis near the sun direction, since the character of the sheath in the vicinity of the terminator is not well understood. Preliminary results of the model calculations are shown in Figure 2. These indicate that (1) the magnitude of the sphere potential difference caused by sheath effects is very dependent on the ambient temperature and density; (2) a reversal of the phase of the observed signal is possible as temperatures increase; (3) as the density becomes progressively lower, the sheath effects first become significant in the negative mode, then may become positive and subsequently saturate in the negative mode; (4) at high densities and low temperatures no sheath effect exists; and (5) saturation occurs at densities (5 to 50) typically seen at the plasmapause boundary (Chappel et al. 1970). The magnitudes of each quantity should only be considered representative as various parameters in the model (e.g. the photoemission from the spheres, photoemission from the body, coupling between the two parts of the body, energy of the photoelectrons, and temperature of the plasma ions compared with the electrons) are only known within reasonable limits and can be adjusted to vary the details of the fit to the data. The general results of the model calculation (regardless of the variations permitted in the aforementioned parameters) do qualitatively explain the observations of potential differences made with S^3_-A at high altitudes. It should be emphasized that these effects occur even though we have assumed complete symmetry in the sensors.

Figure 3 depicts data from the inbound portion of orbit 99, December 16, 1971. The broadband VLF data from the University of Minnesota sensors (magnetic field) and University of Iowa sensors (electric field)

shows that a strong ELF band and whistlers (vertical lines below about 3 kHz in the compressed presentation) begin at the point where our detector comes out of saturation, indicating a definite physical boundary in the medium. At higher L values banded VLF noise is seen. Similar physical boundaries in the broadband data have been correlated with other double probe saturation points. This type of physical boundary in broadband data has been identified as occurring at the plasmapause by comparison to ion data (Carpenter et al. 1969). Thus the identification with the plasmapause of the point where our detector saturates is reasonable in terms of the model and VLF correlations, bearing in mind that the density and temperature combination that is being singled out is not unique, making the identification qualitative.

Accepting this premise, we have studied the orbits in the vicinity of the December 17, 1971, storm to determine the behavior of the plasmapause in this period. Figure 4 depicts the SSS-A orbit and the observed boundaries of the plasmapause for five orbits during and after the main phase of the storm. The shape of the boundary at the crossing is subjective and has been drawn approximately parallel to Carpenter's average plasmapause boundary (Carpenter, 1966), shown in the figure.

In the dusk region on the outbound leg the boundary was often observed several times suggesting that the satellite was on the edge of the bulge or crossed some detached regions of plasma (Chappel et al. 1970). Near midnight the plasmapause is seen to relax outward as the storm activity decreased (see Cahill, 1972, for magnetic behavior in this period). This is portrayed more clearly in Figure 5, which covers the time before the first sudden commencement until well after the recovery phase. In

the midnight sector the boundary was pushed far inward on orbit 99 in response to the first storm activity, relaxed outward during orbit 100 and then was driven in again as the main phase began in orbit 101. The recovery is subsequently steadily outward except in orbits 104 and 106 which were influenced by substorm activity (as seen from high latitude magnetograms). The behavior in the dusk quadrant is more complicated. The double points indicate multiple boundaries. Note that a change in earth radius of the boundary also represents a change in local time since the positions of the measurements are constrained to the orbit of the satellite. Carpenter (1970), using whistlers, has shown the bulge to be displaced sunward during storms and to be co-rotated back in quieting times. The apparent movement in R_e we have observed may be caused either by the shrinking of the total size of the plasmasphere or from longitudinal motions. The minimum radius in the dusk sector occurs well after the minimum radius in the midnight sector. This delay in the dusk profile minimum with respect to that of the nighttime quandrant is suggestive of a co-rotational effect as proposed by Carpenter et al. (1969). Thus the behavior of the plasmapause as detected by the double probe is generally similar to the results of previous studies involving variable magnetic activity, referenced above.

The location of the plasmapause during this storm has been used by Williams et al. (1972) to look at wave particle interactions involving the ion-cyclotron instability. Their study has involved specifically orbit 99, for which our data are shown in Figure 3. Although sheath potentials prevented the DC electric field measurements in this region,

a three channel spectrometer, included to look at the electric field component of waves in the 1-30 Hz range in half decade steps, allowed AC measurements over part of this region. Figure 6 shows the available data from these channels. The enhancement of noise in the region of the plasmapause where the instability is working (especially in the 1-3 Hz band) is expected from Williams' et al. calculations of the ion cyclotron instability. Comparison to Figure 3 shows that the increase to above 100 μv/m occurs coincident with the double probe and broadband detection of the plasmapause. Only the electric field is portrayed, hence, the waves may be either electromagnetic (as appropriate for the ion cyclotron instability) or electrostatic.

Acknowledgment

We wish to thank Dr. L. J. Cahill, Jr., for the magnetic field broadband data and Dr. D. A. Gurnett for the electric field broadband data used in Figure 3, and other cases to help identify the plasmapause.

FIGURE CAPTIONS

Figure 1: Raw data from orbit 110 outbound portraying the two types of sheath potential effects (center and right expanded inserts) including the region of saturation, and the region (left expanded insert) where the measurement of electric fields is free from sheath effects.

Figure 2: Preliminary results of model calculations depicting the effects of ambient electron temperature and density on the measured potentials (see text).

Figure 3: Comparison of the appearance of ELF noise and whistlers and the disappearance of the VLF banded noise with the point of de-saturation of the electric field detector which we are identifying as the plasmapause.

Figure 4: Location of the plasmapause boundaries as defined by the electric field detector during and after the main phase of the December 17, 1971, storm. The shape of the boundary is subjective and has been drawn approximately parallel to Carpenter's (1966) average plasmapause sketched in the figure. The labels are orbit numbers.

Figure 5: A summary of the plasmapause behavior just prior to, during and after the December 17, 1971, storm. Note that an inward motion of the boundary in the evening sector also involves a shift in the observing region toward earlier local times while an inward motion in the night sector involves a shift in the observing location toward later local times

(see Figure 4 for orbit). The x denotes the inbound leg of orbit 97 which remained inside the plasmapause during the whole orbit. The arrows denote the times of the sudden commencements. A and K indices for Fredericksburg are plotted at the bottom of the figure.

Figure 6: Noise observed in the 1-30 Hz range in the region of the plasmapause on orbit 99.

REFERENCES

Cahill, L. J., Jr., Magnetic storm inflation in the evening sector, J. Geophys. Res. 77, this issue, 1972.

Carpenter, D. L., Whistler studies of the plasmapause in the magnetosphere, 1, Temporal variations in the position of the knee and some evidence on plasma motions near the knee, J. Geophys. Res., 71, 693, 1966.

Carpenter, D. L., Whistler evidence of the dynamic behavior of the duskside bulge in the plasmasphere, J. Geophy. Res., 75, 3837, 1970.

Carpenter, D. L., C. G. Park, H. A. Taylor, Jr., and H. C. Brinton, Multiexperiment detection of the plasmapause from Eogo satellites and Antarctic ground stations, J. Geophys. Res., 74, 1837, 1969.

Chappel, C. R., K. K. Harris and G. W. Sharp, The morphology of the bulge region of the plasmasphere, J. Geophys. Res., 75, 3848, 1970.

Chappel, C. R., K. K. Harris and G. W. Sharp, Dayside plasmasphere measurements, J. Geophys. Res., 76, 7632, 1971.

Longanecker, G. W., and R. A. Hoffman, S^3A spacecraft and experiment description, J. Geophys. Res., 77, this issue, 1972.

Williams, D. A., T. A. Fritz, and A. Konradi, Observations of proton spectra ($0.6 \leq Ep \leq 300$ Kev) and pitch angle distributions at the plasmapause, J. Geophys. Res., 77, this issue, 1972.

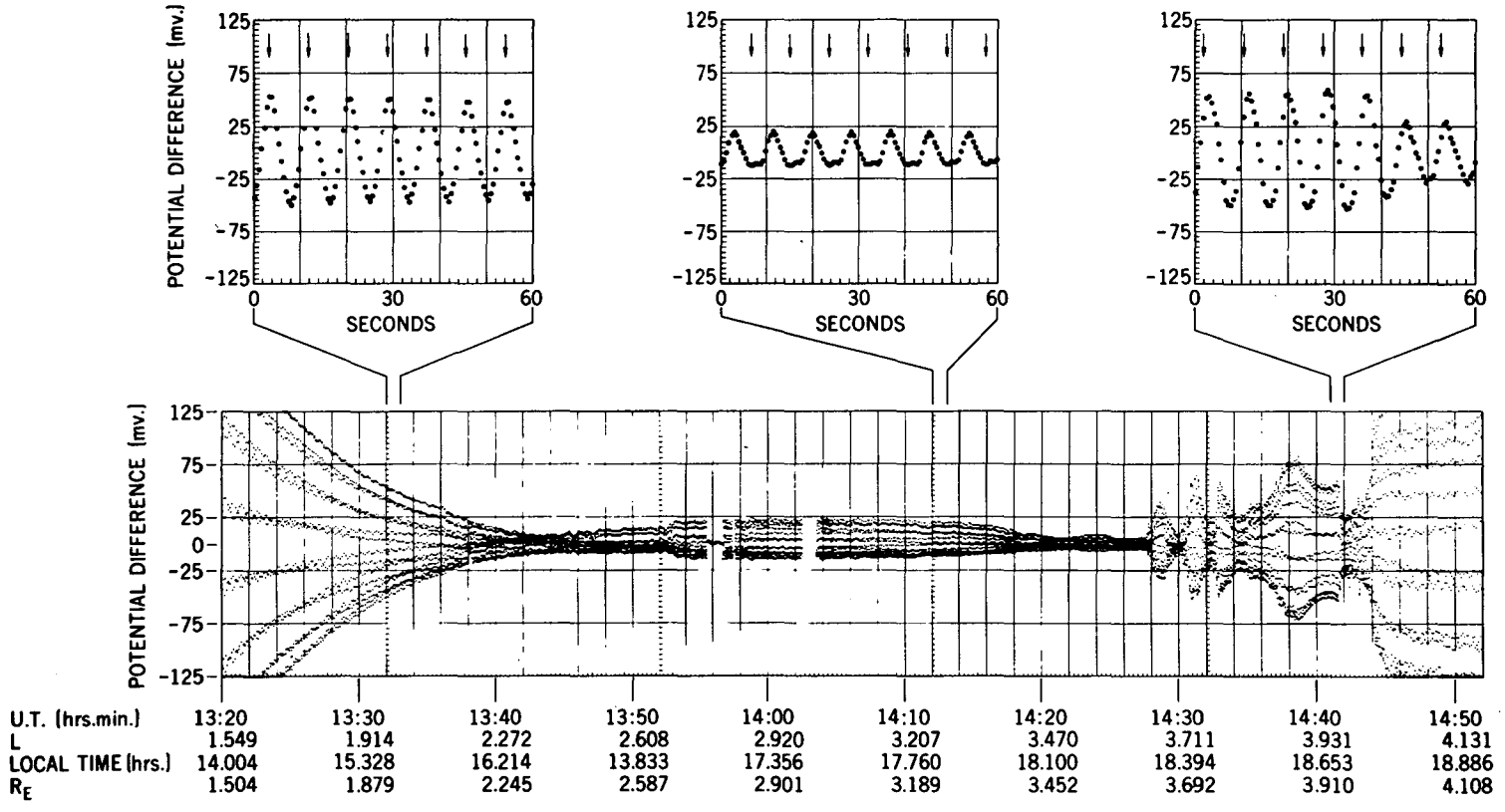
POTENTIAL DIFFERENCE (mv.)
125
75
25
-25
-75
-125
0
30
60
SECONDS
POTENTIAL DIFFERENCE (mv.)
125
75
25
0
-25
-75
-125
U.T. (hrs.min.) 13:20 13:30 13:40 13:50 14:00 14:10 14:20 14:30 14:40 14:50
L 1.549 1.914 2.272 2.608 2.920 3.207 3.470 3.711 3.931 4.131
LOCAL TIME (hrs.) 14.004 15.328 16.214 13.833 17.356 17.760 18.100 18.394 18.653 18.886
R_E 1.504 1.879 2.245 2.587 2.901 3.189 3.452 3.692 3.910 4.108
SSS-A DC ELECTRIC FIELD EXP. ORBIT 110 12/20/71

FIGURE 1

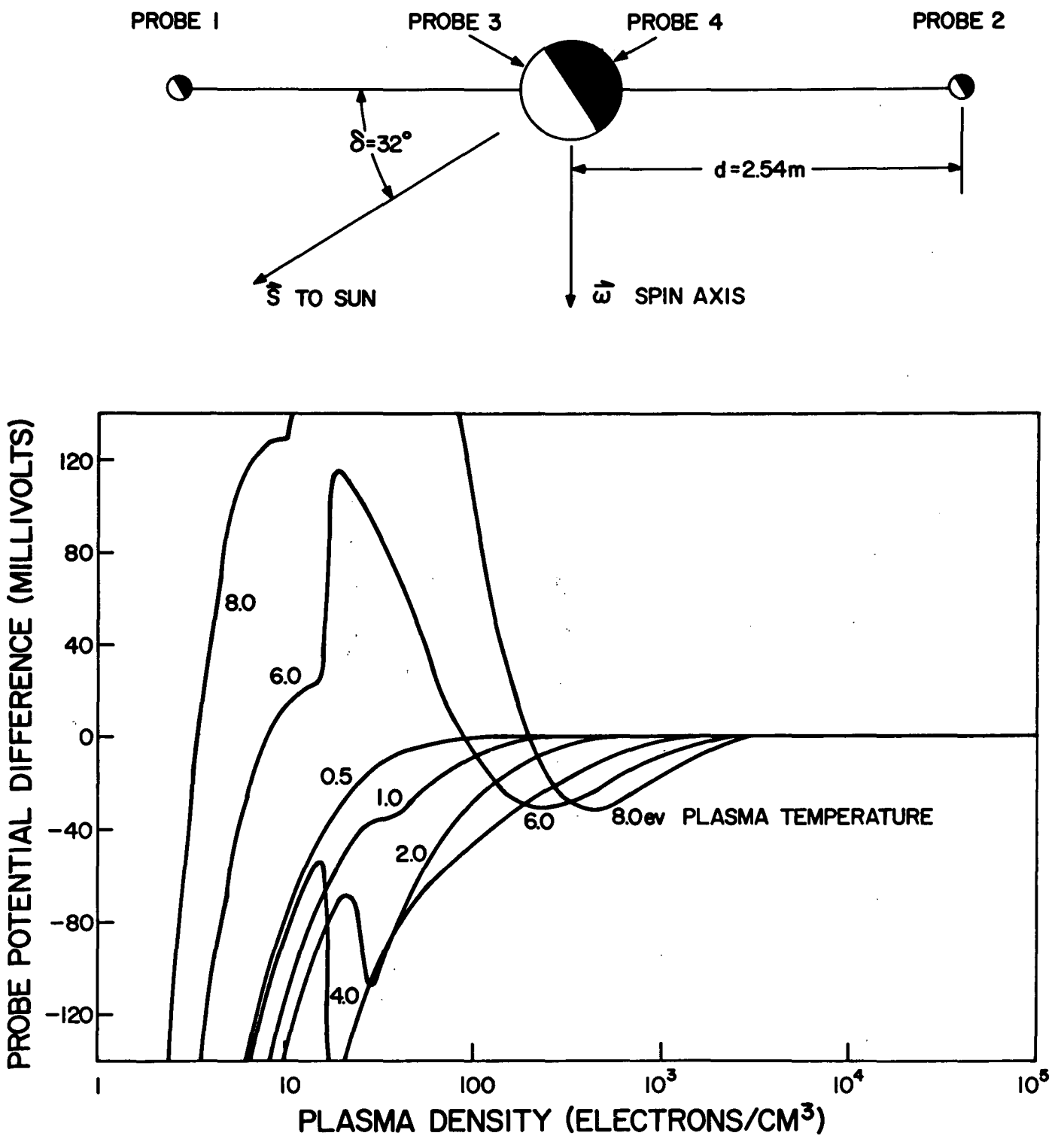
PROBE 1
PROBE 3
PROBE 4
PROBE 2
δ=32°
d=2.54m
$\vec{S}$ TO SUN
$\vec{\omega}$ SPIN AXIS
PROBE POTENTIAL DIFFERENCE (MILLIVOLTS)
120
80
40
0
-40
-80
-120
8.0
6.0
0.5
1.0
2.0
4.0
6.0
8.0ev PLASMA TEMPERATURE
1
10
100
10^3
10^4
10^5
PLASMA DENSITY (ELECTRONS/CM^3)

FIGURE 2

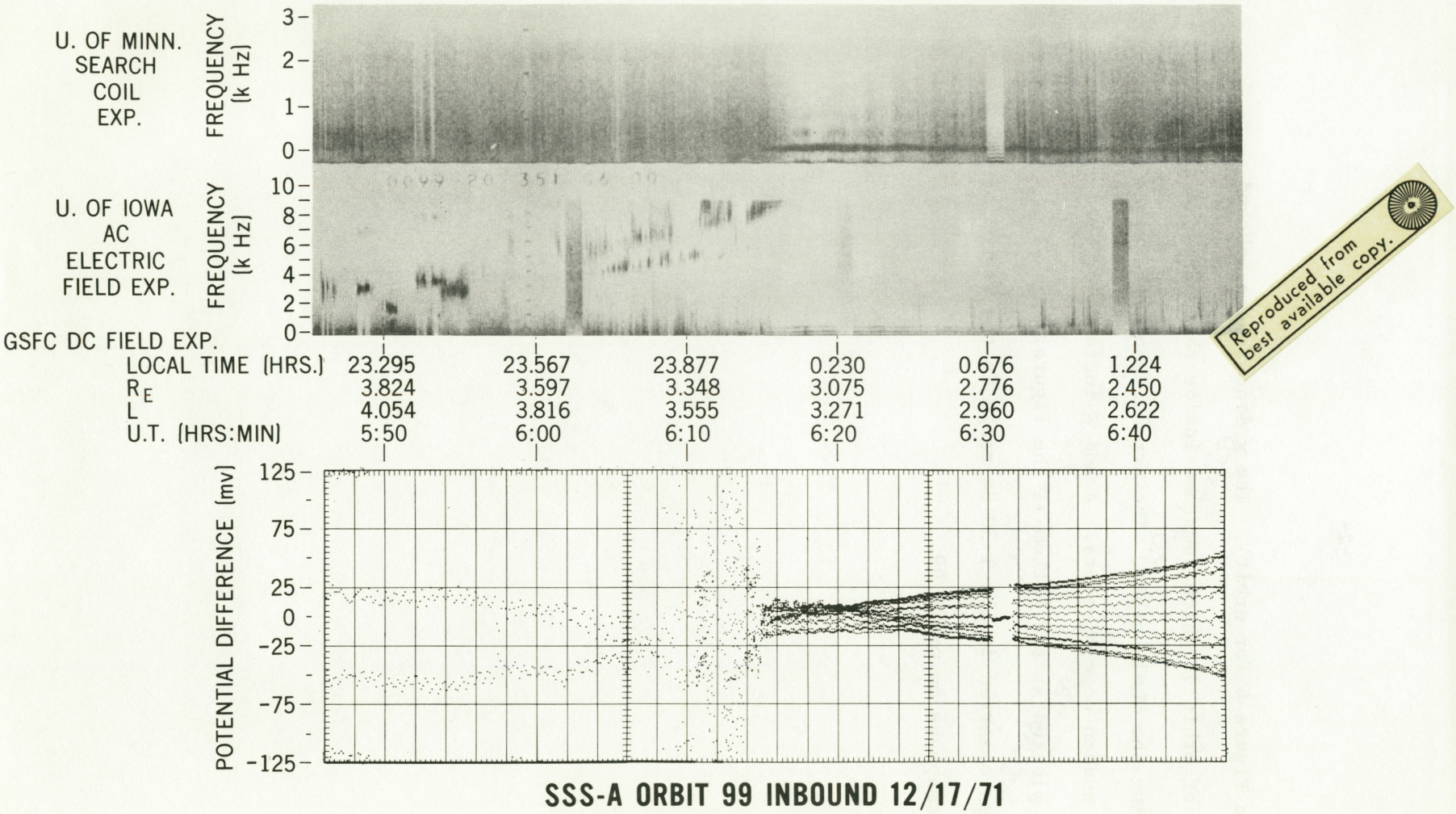

FIGURE 3

(see Figure 4 for orbit). The x denotes the inbound leg of orbit 97 which remained inside the plasmapause during the whole orbit. The arrows denote the times of the sudden commencements. A and K indices for Fredericksburg are plotted at the bottom of the figure.

Figure 6: Noise observed in the 1-30 Hz range in the region of the plasmapause on orbit 99.

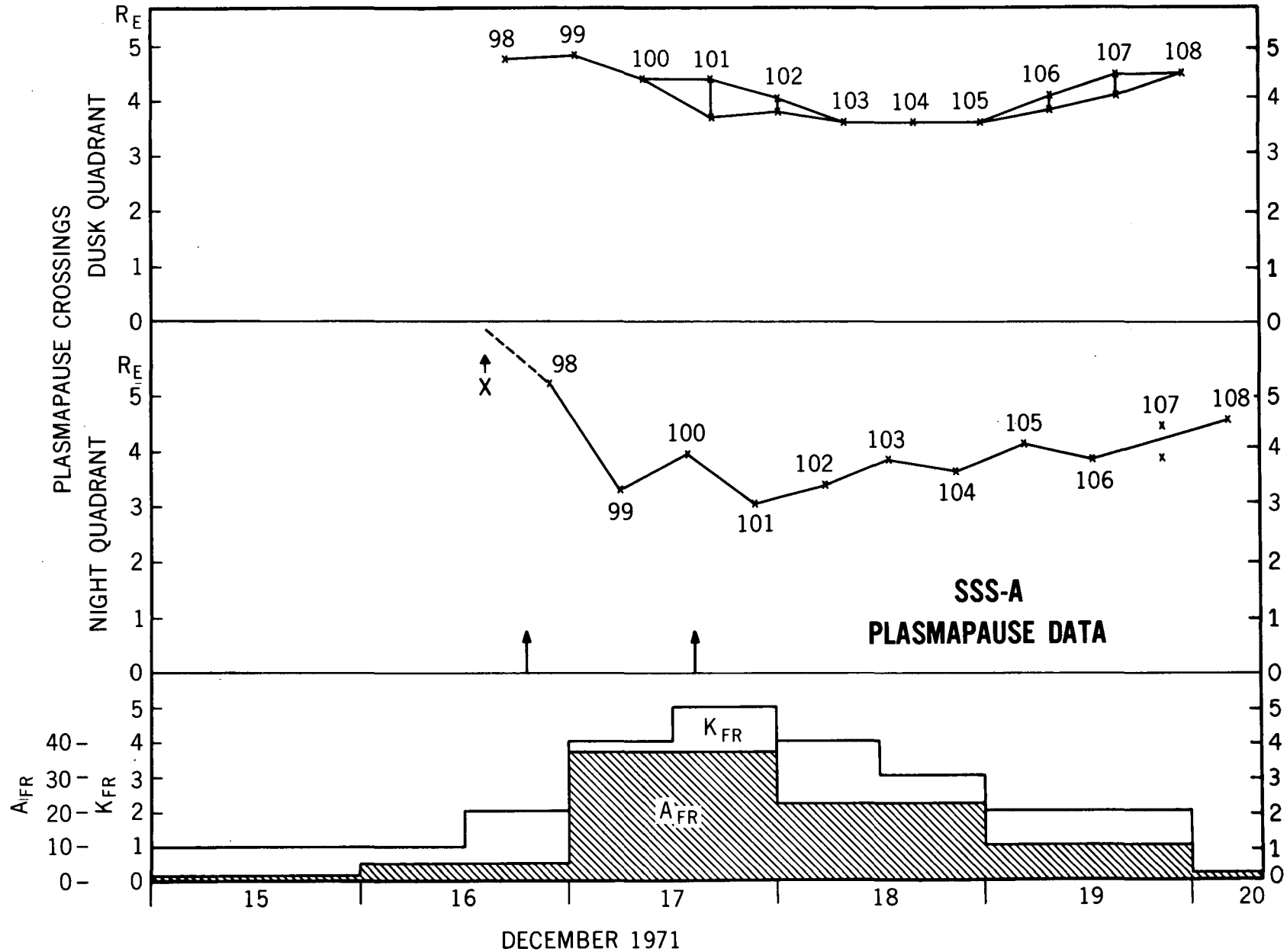
PLASMAPAUSE CROSSINGS
DUSK QUADRANT
NIGHT QUADRANT
R_E
98
99
100
101
102
103
104
105
106
107
108
SSS-A
PLASMAPAUSE DATA
K_{FR}
A_{FR}
40
30
20
10
0
15
16
17
18
19
20
DECEMBER 1971

FIGURE 5

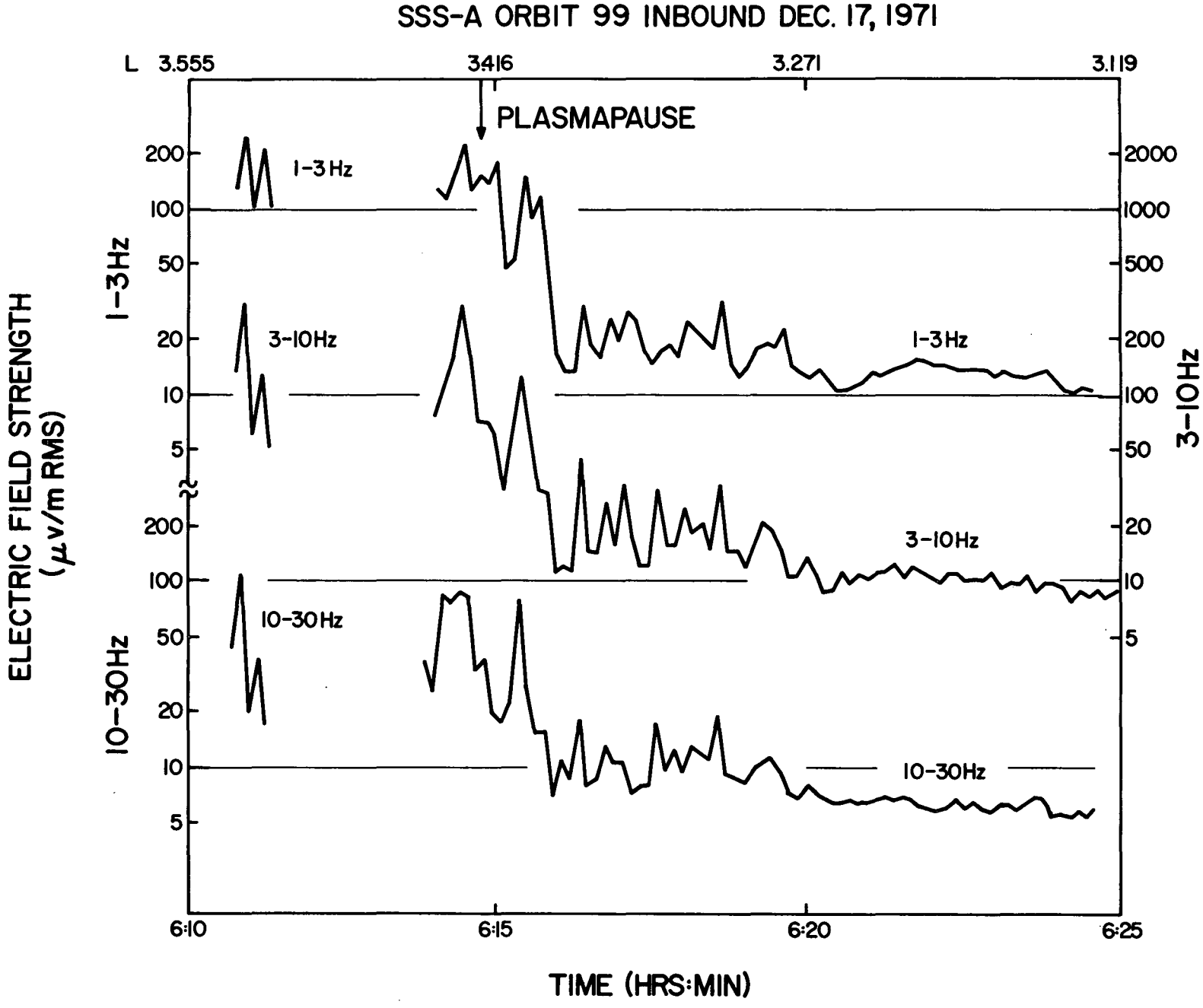
SSS-A ORBIT 99 INBOUND DEC. 17, 1971
L 3.555
3.416
3.271
3.119
PLASMAPAUSE
1-3Hz
3-10Hz
10-30Hz
ELECTRIC FIELD STRENGTH (μv/m RMS)
200
100
50
20
10
5
2000
1000
500
200
100
50
20
10
5
6:10
6:15
6:20
6:25
TIME (HRS:MIN)

FIGURE 6